Algal Research 93 (2026) 104483

Contents lists available at ScienceDirect

Algal Research

journal homepage: www.elsevier.com/locate/algal

Short communication

HPLC quantification of guanine, hypoxanthine, xanthine, and uric acid in microalgae: The effects of different nitrogen sources on the purine profile of *Cryptomonas maculata*

Maximilian Bott *, Anne Jantschke

Institute for Geosciences, Johannes Gutenberg-Universität Mainz, 55122, Mainz, Germany

ARTICLE INFO

Keywords:
Biogenic organic crystals
Solid solution
Crystalline inclusions

ABSTRACT

Microalgae are a substantial group of primary contributors to all aquatic reservoirs on earth. A recently observed strategy in their nitrogen metabolism is the ability to form purine-based crystalline inclusions that are often solid solutions. In microalgae, they are proposed to function as concentrated reservoirs of stable, nitrogen-containing, rapid-turnover metabolites or stress responses. Yet, many aspects in nitrogen-metabolization and compositional dynamics remain unclear.

To address this issue, an HPLC method for the quantification of all relevant purines (guanine, hypoxanthine, xanthine and uric acid) was designed and applied to 14 taxonomically different microalgae. *Cryptomonas maculata* was selected as a model species to study the effects of different nitrogen sources ($NaNO_3$ and urea) at lowered and increased concentrations on purine formation over time. This study is the first to address purine formation in a time-resolved manner and to analyze compositional dynamics.

One of the main results of the study is the high variability in uric acid concentrations, while the concentrations of guanine, xanthine, and hypoxanthine remain constant. The type of nitrogen source is shown to be more impacting on these concentrations than the actual concentration of nitrogen. Further, a significant amount of uric acid was produced during the initial phase of cultivation, followed by its subsequent degradation after 2 to 4 weeks.

These findings offer a first insight into the complex dynamics and responses of microalgae to environmental changes and hold considerable potential to elucidate a wide range of phenomena, including algae blooms and the dynamics of coral ecosystems.

1. Introduction

Guanine is a ubiquitous molecule in nature, serving essential roles through its function as a nucleobase in the complex machinery that stores genetic information as DNA or RNA. Furthermore, it is a crucial component in GTP/GDP where it acts as a signaling molecule in G-protein coupled signaling pathways [1–3]. Guanine fulfills the molecular requirements of these examples by combining an aromatic character and potential hydrogen bonding. It is well examined that, due to these properties, guanine forms stacked planes of hydrogen-bonded molecules during crystallization of both anhydrous polymorphic forms [4,5]. The α-form was determined in synthetic crystals [4], whereas the recently discovered β-form appears in all guanine crystals found in living organisms [5,6].

When the crystals form as thin plates parallel to the hydrogen bonded planes, the refractive index in the direction perpendicular to the plate is extremely high (1.83) [7,8]. This is the reason why guanine crystals are utilized by fish and other animals for the purposes of light manipulation, whereby they produce structural colors, and for vision, whereby they construct mirrors that reflect light [6]. White spiders use guanine crystals with prismatic morphology to scatter light, giving them their white appearance [9].

However, there have been several reports of the presence of guanine crystals produced by organisms that are not animals [10–14]. It is becoming increasingly evident that purine-based crystalline inclusions are ubiquitous among unicellular eukaryotes, rather than a rare phenomenon found in a few individual species [15], which is fostering a growing interest among researchers in their role in ecosystem dynamics.

* Corresponding author.
E-mail address: mbott@uni-mainz.de (M. Bott).

https://doi.org/10.1016/j.algal.2025.104483
Received 23 May 2025; Received in revised form 7 November 2025; Accepted 11 December 2025
Available online 12 December 2025

Jantschke et al. were the first to identify guanine deposits in the dinoflagellate *Calciodinellum operosum aff.* using Raman imaging and 2D/3D-cryo-(FIB)-SEM [16]. Mojzeš et al. found that guanine is widely distributed in various microalgal groups as a high-capacity and fast-turning metabolite [17].

Despite wider investigation, purine-based crystalline inclusions in eukaryotes are not confined to doped arrangements of guanine. In 2009, Clode et al. [18] discovered that crystalline inclusions in the microalgal symbionts of *Aiptasia* sp. that were thought to be oxalic acid were, in fact, uric acid. This finding led to the hypothesis that there is a symbiotic relevance in the N-assimilation of dinoflagellates and their cnidarian host organism, *Aiptasia* sp. anemones. Subsequent research by Kopp et al. [19] provided further evidence for this hypothesis by demonstrating that dinoflagellates exhibit a rapid response to increased nitrogen concentrations, with a prompt uptake and subsequent translocation to its coral host within a few hours.

Some biogenic guanine crystals in animals have been demonstrated to be solid solutions, exhibiting the capacity to incorporate other purines, especially hypoxanthine, while preserving their crystal structure [20]. While it remains to be investigated, it is conceivable that purine crystals in microorganisms may also be solid solutions of multiple purine analogs.

In general, it is well established that the de novo synthesis of all purines in organisms is realized by a highly conserved gene cluster, the IMP-*de novo* synthesis [21] In this process, the purines are not formed as free molecules, but as nucleotides, utilizing a ribose 5-phosphate backbone. Upon degradation, the nucleotides are dephosphorylated to nucleosides and subsequently cleaved of the ribose-analog employing a purine nucleosidase phosphorylase to yield the purines hypoxanthine and guanine (Fig. 1). The transformation of both molecules to xanthine is catalyzed by a xanthine oxidase or guanine deaminase respectively. Subsequently, xanthine oxidase catalyzed the oxidation of xanthine to uric acid. Depending on the organism, uric acid is either further processed or excreted.

The composition of these crystals in microalgae was identified by Raman microscopy [14,15] or TEM [18] but not quantified. Consequently, there is a clear requirement for the development of a method for the precise and rapid quantification of the individual purines and dopants within the crystalline inclusions. Although the function and structural characteristics of numerous examples in higher order animals are well understood and examined, the nitrogen-metabolization and compositional dynamics in microalgae, remain unclear.

To address this, an HPLC method for the quantification of guanine, hypoxanthine, xanthine and uric acid was developed. This method was then applied to 14 taxonomically different microalgae. *Cryptomonas maculata* (*C. maculata*) was used as a model species for further analysis due to its comprehensive purine profile. The effect of the use of different nitrogen sources as well as increased and decreased nitrogen concentrations on the purine profile of *C. maculata* was examined by HPLC.

2. Materials and methods

A full list of chemicals used in this study, details on algal cultivation, as well as HPLC sample preparation and measurement details and micro-Raman spectroscopy, are provided in the Supplementary Information.

3. Results and discussion

3.1. Method validation

The HPLC quantification method is based on the protocol developed by Fan et al. [26] for the fungus *Cordyceps*. For the total quantification of purines in microalgae, the scope of the method was extended to include the additional analytes uric acid and xanthine. The pyrimidine bases thymine, uracil, and cytosine that were analytes in the original method, were not monitored during this work. Furthermore, the mobile phase was changed from aqueous TEA to formate buffer to prolong the lifetime of the column as it is not intended for use above pH 8. The method was optimized with respect to column temperature (in the range of 25–40 °C) and flow rate (in the range of 0.3–1.0 mL/min) to achieve optimal analyte separation. Calibrations were performed using 8 to 11 concentrations of the respective analytes and a fixed concentration of 43.3 ng/mL allopurinol as an internal standard. All calibration curves are shown in the supplementary information. (SI, Fig. S1).

The specificity of the method was ensured by correlating the retention times of all analytes with separately measured analyte standards (Fig. 2A). Further, the DAD detector of the HPLC system allowed a direct comparison of the UV–Vis spectra of all analytes (in the range of 200–400 nm). Characteristic absorption maxima are observed for the analytes and were used to identify signals in the chromatogram. Samples in which no analyte was detected exhibited no absorption at the corresponding retention time.

The linearity and regression of the method was validated by the correlation coefficients ($r^2 > 0.999$) of all four analytes (Table 1). This indicates a precise correlation between the analyte concentrations and their measured peak areas. For all analytes, the limit of detection (LOD) and limit of quantification (LOQ) were determined to be lower than 1 µg/mL and 2.8 µg/mL (Table 1, determined for uric acid). The obtained LOD and LOQ for hypoxanthine and guanine are thereby consistent with the original method.

As indicated in previous studies, analyte concentrations can decline over time, which may be caused by degradation resulting from the

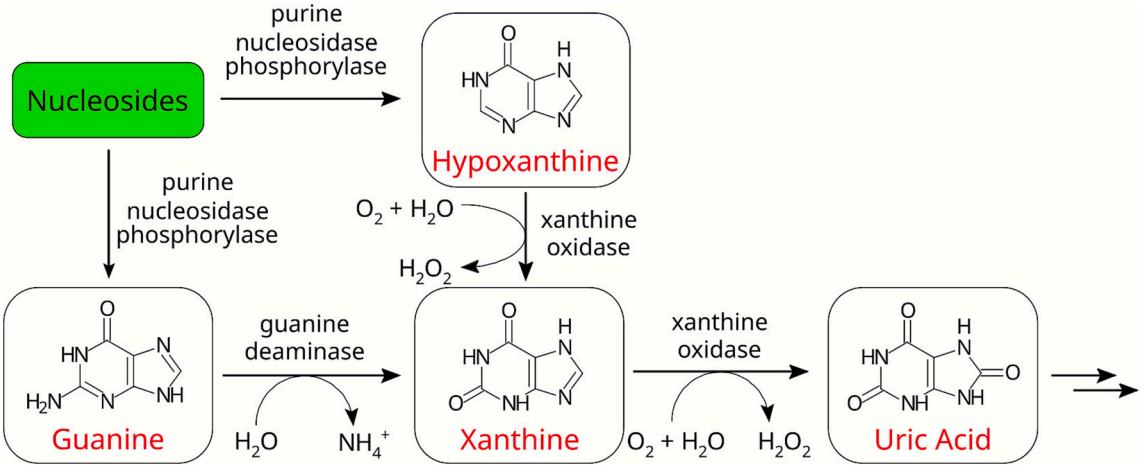

Fig. 1. Schematic nucleoside degradation and involved enzymes adapted from Biochemie und Molekularbiologie [22].

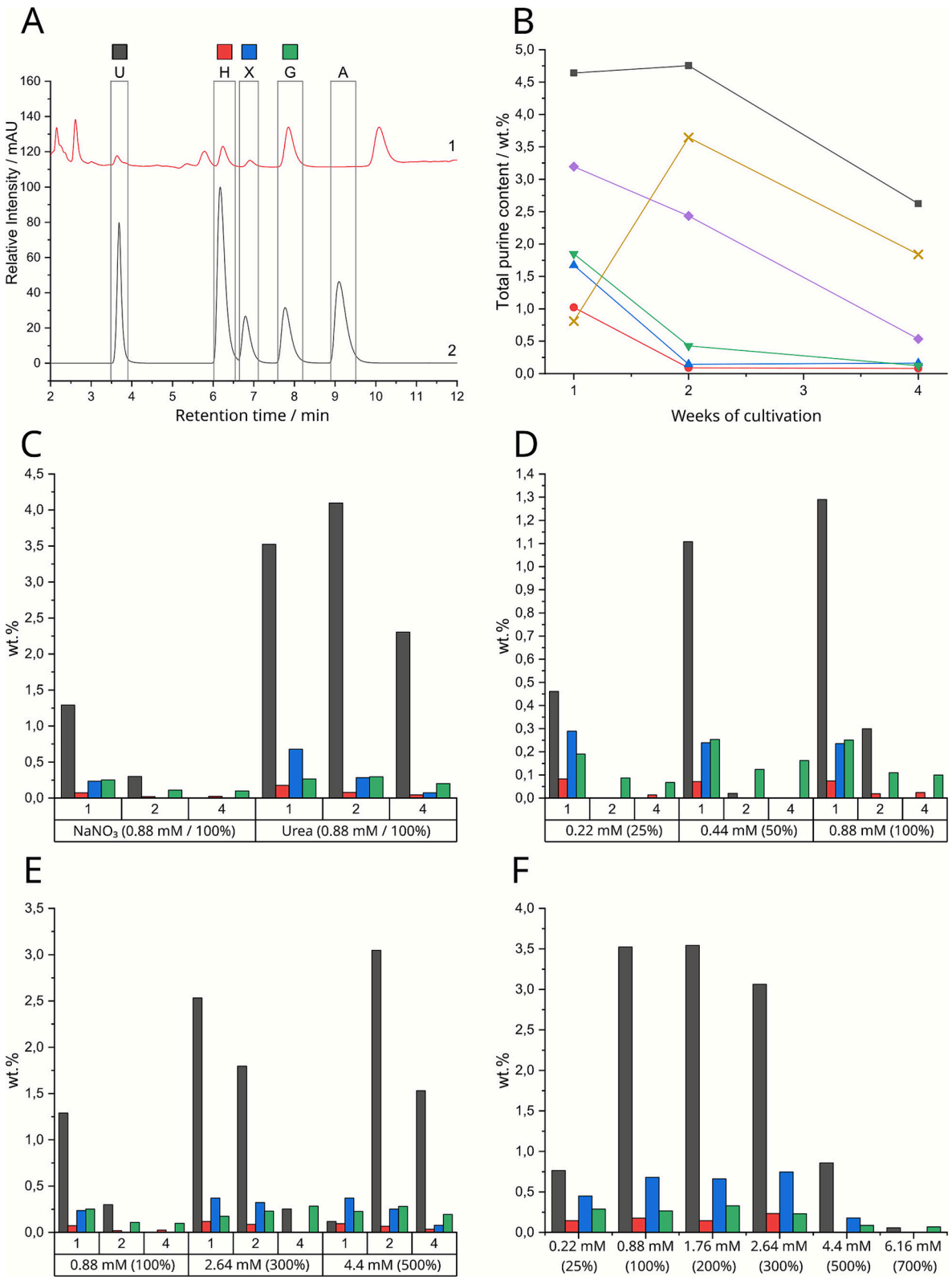

Fig. 2. A) Chromatograms of (1, red) extract of *Cryptomonas maculata*, displayed with an offset of 110 mAU and (2, black) mixture of uric acid (U, grey), hypoxanthine (H, red), xanthine (X, blue), guanine (G, green), and allantoin (A) measured at 250 nm. **B)** Total purine content in wt% after 1, 2, and 4 weeks at 0.22 mM (= 25 %; ●), 0.44 mM (= 50 %; ▲), 0.88 mM (= 100 %; ▼), 2.64 mM (= 300 %; ◆) and 4.4 mM (= 500 %; ✖) $NaNO_3$ and 0.88 mM (= 100 %; ■) urea. (For interpretation of the references to colour in this figure legend, the reader is referred to the web version of this article.)
HPLC results of *C. maculata* **C)** Cultivated for 1, 2, and 4 weeks at 0.88 mM (= 100 %) urea and $NaNO_3$. **D)** cultivated for 1, 2, and 4 weeks at 0.22 mM (= 25 %), 0.44 mM (= 50 %) and 0.88 mM (= 100 %) $NaNO_3$. **E)** cultivated for 1, 2, and 4 weeks at 0.88 mM (= 100 %), 2.64 mM (= 300 %) and 4.4 mM (= 500 %) $NaNO_3$. **F)** cultivated for 1 week at 0.22 mM (= 25 %), 0.88 mM (= 100 %), 1.76 mM (= 200 %), 2.64 mM (= 300 %), 4.4 mM (= 500 %), and 6.16 mM (= 700 %) urea. Measured contents of uric acid (U, grey), hypoxanthine (H, red), xanthine (X, blue), and guanine (G, green) are displayed in wt% to the freeze-dried material. Please note that figures B) – F) are displayed with varying y-axes.

Table 1
Linear regression table with linear range, regression equation, r^2 COD (coefficient of determination), LOD (limit of detection) and LOQ (limit of quantification) for all quantified analytes.

Analytes	Linear regression			LOD (µg/mL)	LOQ (µg/mL)
	Linear range (µg/mL)	Regression equation	r^2		
Hypoxanthine	0.25–5.05	y = 0.297× – 0.005	0.9997	0.102	0.308
Xanthine	0.25–9.8	y = 0.18× + 0.011	0.9995	0.272	0.825
Guanine	0.06–1.4	y = 0.683× – 0.004	0.9992	0.045	0.135
Uric Acid	0.67–90.45	y = 0.52× – 0.02	0.9999	0.924	2.799

perchloric acid treatment [26,27]. To test this, each analyte was incubated with concentrated perchloric acid (70 %) using the same procedure as for the algae samples. The corresponding UV–Vis spectra were monitored over time (up to 4 h, SI, Fig. S2). The absorption spectra of guanine, xanthine and hypoxanthine show no degradation or transformation even after 4 h. For uric acid, a small decline in the absorption maximum at 300 nm was observed after 4 h, suggesting a minor degree of degradation over time. This appears logical, given the anti-oxidative characteristics of uric acid in the strong oxidative environment of perchloric acid [28,29] Consequently, the HPLC-detected uric acid (after 1 h of PCA incubation) may be underdetermined.

3.2. Quantification of purine-bases in microalgae

To evaluate the efficacy of the optimized quantification method, we selected 14 species of phylogenetically different microalgae for cultivation (SI, Table S1) and compared their HPLC purine profiles to the comprehensive Raman data set presented by Pilátová et al. [15] after a four-week cultivation period (Table 2). An exemplary HPLC plot is shown in the supplementary information. (SI, Fig. S3) It is important to note that all measured purine concentrations refer to the total amount of purines in the whole cell, not just the crystalline inclusions.

All screened species exhibited **guanine** contents ranging from 0.09 wt% to 1.43 wt%, which was expected as all living cells incorporate guanine in their DNA. Here, the highest contents were observed in the examined alveolate species, which were all members of the Dinophyceae class [14,16,17]. *Thoracosphaera heimii* and *Calciodinellum operosum* exhibited the lowest amounts among the Alveolata clade (≈ 0.55 wt%), yet this was approx. twofold more than the highest amounts detected among all other species (≈ 0.23 wt%).

Table 2
Screened species and their guanine, hypoxanthine, and xanthine content quantified by HPLC analysis.

Phylum	Species	Guanine / wt%	Hypoxanthine / wt%	Xanthine / wt%
Stramenopiles	*Navicula* sp.	0.183	–	–
	Nannochloropsis sp.	0.157	–	–
Archaeplastida	*Chlorella vulgaris*	0.223	–	–
	Chlorella angusto ellipsioedea	0.238	–	–
	Tetraselmis suecica	0.089	–	–
Cyanophyceae	*Synechococcus* sp.	0.146	–	–
Haptista	*Isochrysis galbana*	0.221	–	0.018
Cryptophyceae	*Cryptomonas maculata*	0.227	0.051	0.015
	Chroomonas sp.	0.404	–	–
Alveolata	*Leonella granifera*	1.429	0.023	–
	Thoracosphaera heimii	0.535	0.019	–
	Calciodinellum operosum	0.569	0.012	–
	Scrippsiella trochoidea	0.805	–	–
	Symbiodinium voratum	0.642	–	–

Hypoxanthine could be identified in four species with concentrations ranging from 0.01 wt% to 0.05 wt%. **Xanthine** was found only in *Isocrysis galbana* and *Cryptomonas maculata* (*C. maculata*) with a content of approx. 0.02 wt%. These two purines are known dopants of crystalline guanine deposits of higher order animals [20], but the functional roles and dynamics of these dopants in the crystalline deposits remain unclear. **Uric acid** was not found in any of the analyzed species.

Surprisingly, some of the results support the findings of Pilátová et al. [15] while others show different purine patterns: For example, based on their Raman screening of >200 eukaryotic organisms, xanthine crystals were only rarely observed in species of the clade Archaeplastida, or the phyla Haptista, and Amoebozoa such as *Chlorella vulgaris* and *Isocrysis galbana*, a result that couldn't be reproduced by the HPLC analysis. According to Pilátová et al. [15], *Cryptomonas* sp. formed uric acid crystals, whereas the HPLC analysis of *C. maculata* after 4 weeks cultivation time showed no uric acid, but hypoxanthine and xanthine. Similarly, *Chlorella vulgaris*, *Tetraselmis subcordiformis*, and *Isochrysis* sp. have all been reported to form additional purines in addition to guanine [15], but HPLC quantification after 4 weeks cultivation showed guanine only. However, the results for *Nannochloropsis* sp. were found to be consistent, with only guanine detected in this species. These discrepancies may be partially explained by the different time points of investigation. Pilátová et al. [15] typically obtained their results a few days after incubations, whereas in our case, after 4 weeks the cells probably reached the stationary phase. These results underscore the need for a time-resolved analysis of purine levels in relation to the cell's physiological conditions.

To address these inconsistent findings and to determine the nitrogen conditions that induce changes in purine profiles, *C. maculata* was selected for further analysis as it was the only species that formed guanine, hypoxanthine and xanthine simultaneously. To track purine formation and its dynamics, *C. maculata* was incubated with urea and nitrate at varying nitrogen concentrations and the purine profiles were analyzed over time.

3.3. Variation of nitrogen source (NO_3^- vs urea)

Nutritional fluctuations occur constantly in marine environments. Here nitrogen-containing compounds play a crucial role in the metabolic flux of primary contributors. As such, microalgae cope with these fluctuations by changes in their growth dynamics [30–35] and/or the formation of various compounds, such as lipids [31,36–38], carbohydrates [39–41], or carotenoids [42,43].

However, the effect of different nitrogen-containing compounds on purine formation in microalgae has not been systematically studied yet. To address this, *C. maculata* cultures were incubated with the two naturally occurring nitrogen sources $NaNO_3$ and urea (0.88 mM) and harvested after 1, 2, and 4 weeks. Ammonium chloride was also tested as a potential nitrogen source, but *C. maculata* did not tolerate NH_4Cl even at low concentrations (SI, Fig. S4).

The total amount of purines (Fig. 2B) decreased constantly in the nitrate containing culture from approximately 1.8 wt% after week 1 to 0.4 wt% after week 2 and 0.1 wt% after week 4. In contrast, the purine content of the urea containing culture slightly increased from 4.6 wt% after week 1 to 4.7 wt% after week 2. After 4 weeks, the total purine content in the urea containing medium decreased to 2.7 wt%. Consequently, the trend of initial purine formation with subsequent degradation becomes apparent for both nitrogen species. Even though urea contains twice the number of nitrogen atoms per molecule compared to nitrate, an even greater quantity of purines was formed. One potential explanation for this phenomenon could be attributed to the higher bioavailability of urea for *C. maculata*. Alternatively, a delayed

accumulation of uric acid in the urea-containing medium could be a contributing factor. Under this assumption, the culture containing nitrate had already entered the degradation phase by week 1, while the culture with urea was still in the accumulation phase. It is important to note that the effects of nitrate and urea on the enzymatic activity relevant to purine formation have not been examined systematically in this or previous studies.

When comparing the different nitrogen sources, the resulting purine profiles were notably different (Fig. 2C). After week 1, *C. maculata* grown with urea formed more than twice the amount of uric acid, hypoxanthine and xanthine. The concentrations of these three purines decreased over the course of 4 weeks, except for the uric acid concentration in the urea containing medium, which increased after week 1 but decreased subsequently after week 2. In contrast, the guanine concentration was found to remain relatively constant at approx. 0.25 wt% in the urea containing medium.

3.4. Increase and decrease of NO_3^-

Just as the species of nitrogen containing compounds varies in natural marine environments, so does their concentration. Microalgae must respond to these fluctuations in a dynamic manner, yet the mechanisms by which they cope with nutrition deficiencies and excesses were never investigated with respect to their purine profile. To identify these responses, *C. maculata* cultures were incubated with different concentrations of nitrate, ranging from 0.22 mM (equivalent to 25 %) to 4.4 mM (equivalent to 500 %). The resulting purine profiles of decreased (Fig. 2D) and increased (Fig. 2E) nitrate levels were then compared to the original growing condition of 0.88 mM (equivalent to 100 %) NO_3^-.

At decreased nitrate concentrations (Fig. 2D), similar levels of xanthine (≈ 0.26 wt%), guanine (≈ 0.25 wt%) and hypoxanthine (≈ 0.08 wt%) were observed after week 1. In contrast, a significant difference was observed in the uric acid levels: both the 50 % and 100 % culture contained about 2.5-fold more uric acid (1.2 wt%) compared to the culture containing only 25 % (0.45 wt%). After 2 and 4 weeks, no xanthine could be identified, and guanine levels decreased by half but remained constant at approximately 0.1 wt%. Hypoxanthine contents were observed inconsistently but lowered to about 25 % of the initial, week 1 concentration, if observed. Uric acid was not detected after week 2 in the 25 % sample and only traces remained in the 50 % sample. In contrast, the 100 % sample exhibited about 25 % of the initial week 1 concentration. None of the cultures exhibited uric acid after 4 weeks of cultivation.

After week 1 at increased nitrate concentrations (Fig. 2E), comparable trends to the observations at reduced concentrations were evident. The levels of xanthine, hypoxanthine and guanine remained consistent across all concentrations ranging from 100 % to 500 %. At 300 % and 500 %, these concentrations stayed constant until week 2 before declining after week 4. Moreover, the 500 % culture was the only sample to contain xanthine after 4 weeks. For uric acid, the 100 % and 300 % cultures exhibited comparable trends of uric acid levels as they decreased over time, had a maximum after the first week, and correlated to the concentration of nitrate. Only the 500 % sample exhibited a notably low amount of uric acid (≈ 0.1 wt%) in week 1, which increased to approximately 3 wt% by week 2. This delay in uric acid formation suggests that high nitrate concentrations may influence either the xanthine oxidase activity, expression, or a different step in the corresponding metabolic pathway.

3.5. Increase and decrease of urea

In a similar manner, *C. maculata* cultures were studied at varying urea levels. Due to the vast utilization of urea-based fertilizers in nowadays agriculture, some coastal areas suffer from the effects of urea pollution and their contribution to the formation of harmful algae blooms [35,44]. A few decades ago, the effects of urea on nitrogen metabolism were explored when *Chlorella ellipsoidea* and *Prorocentrum micans* were observed to excrete ammonia when cultivated with urea [45]. This appears logical, as various members of the Bacillariophyceae [46], Cyanophyceae [47,48], Prasinophyceae [46], Chrysophyceae [46,49], and Xanthophyceae [46,50] are known to assimilate urea by their urease activity. In addition to ammonia, the microalgae *Scenedesmus* sp. [51] and *Chlorella* sp. [52–54] excrete various amino acids, including glutamic acid, glutamine, alanine, and arginine, which are products of the ornithine cycle. Yet, to the best of our knowledge, no study has ever examined altercations in purine production.

To address this issue and to put the effect of different nitrogen sources further into perspective, *C. maculata* cultures were incubated at varying urea levels and analyzed by HPLC after week 1 of cultivation (Fig. 2F). Cultures cultivated at 100 %–300 % urea formed almost identical purine profiles containing approx. 3.0–3.5 wt% uric acid, 0.1 wt% hypoxanthine, 0.7 wt% xanthine and 0.5 wt% guanine. Surprisingly, the 25 % urea culture formed similar amounts of hypoxanthine, xanthine and guanine with a reduced uric acid level of 0.8 wt%. This finding might indicate the presence of distinct levels of control over the metabolic intermediates of purines, where guanine, hypoxanthine, and xanthine could be regarded as intermediates with highly regulated concentrations. Conversely, uric acid functions as the "storage molecule", accumulating initially and subsequently undergoing transformation. Strongly elevated urea concentrations (500 % and 700 %) resulted in a visible manifestation of cellular stress, as evidenced by a paler cell appearance and a concomitant reduction in autofluorescence. This stress was accompanied by a significant decline in purine production (total purine content <1.1 and 0.2 wt.-%). Although this was unexpected, given that *C. maculata* is capable of assimilating urea, it was also reported by Johnson [55], who cultivated *Rhodomonas lens* in seawater with varying levels of urea. Based on an increase in pH to 9.2 at the end of cultivation in combination with the urease activity established for Chrysophyceae, it was hypothesized that the stress and subsequent cell lysis of *Rhodomonas lens* was caused by ammonia toxification. As a control, the pH was artificially increased using NaOH, which did not lead to any stressed or malformed cells and did not produce comparable effects. It is therefore logical to infer that ammonia, which is formed by the degradation of urea, is rapidly metabolized and assimilated further. However, at a certain concentration of urea, the produced ammonia, or other metabolic by-products, are not sufficiently degraded, which results in toxification and subsequently cell death. The discrepancy between the measured amounts of purines and the actual amount of urea remains a subject for further research.

3.6. Micro-Raman spectroscopy

Micro-Raman spectroscopy is a powerful tool to analyze the intracellular distributions of cellular constituents and distinguish different purine bases [15–17]. Raman analysis of *C. maculata* reveals distinct Raman signatures of starch, lipids and seawater, as well as purine inclusions (full spectra in the SI, Fig. S5) which are visualized in Fig. 3.

The Raman maps of Fig. 3A clearly show that the purine inclusions are localised intracellularly within individual, small compartments. The Raman spectrum obtained for these purine inclusions is shown in Fig. 3B. The purine skeletal vibration is observed at ~630 cm^{-1}, which is characteristic of uric acid [56,57]. Previous studies have observed this mode at wavenumbers below 630 cm^{-1} [15,57,58], which is indicative of anhydrous uric acid. In *C. maculata,* however, the band is shifted to higher wavenumbers with a band at 634 cm^{-1}, which indicates the presence of a hydrated urate, such as monosodium urate hydrate or ammonium urate hydrate [56,59]. Raman analysis shows no difference between the different nitrogen conditions.

4. Conclusions

By establishing a method for the precise total quantification of

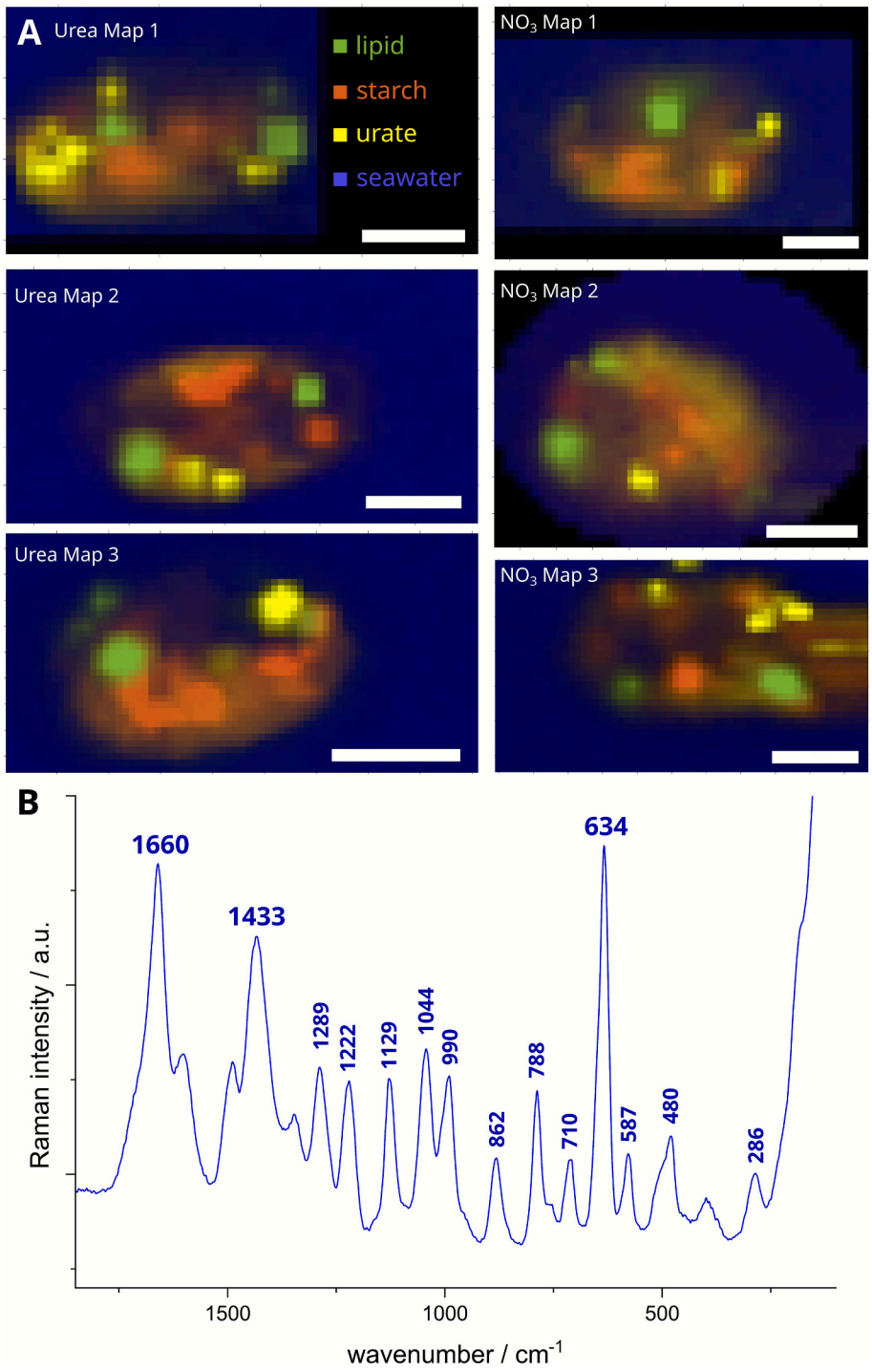

Fig. 3. Micro-Raman spectroscopy of individual cells of *C. maculata* using urea and nitrate as nitrogen source (0.88 mM) after 2 weeks of cultivation. A) Raman maps showing the distribution of the identified cellular components lipids (green), starch (orange), urate crystals (yellow) and seawater (blue). B) Average Raman spectrum of the crystalline purine inclusions (total: 25 spectra). (For interpretation of the references to colour in this figure legend, the reader is referred to the web version of this article.)

guanine, hypoxanthine, xanthine and uric acid in microalgae, this study has demonstrated that the purine profiles in *Cryptomonas maculata* are highly dynamic and change more by type of available nitrogen source, than their actual concentration. Additionally, the concentration of purines is significantly dependent on the cultivation time and declines after their initial increase. It is important to note that all measured purine concentrations refer to total amounts in whole cells. Future research will address the precise composition of crystalline purine inclusions following extraction.

These findings are thereby expected to be representative of other algae of the Pyrenomonadales order or even the whole Cryptophyceae class. Yet, it cannot be assumed that *C. maculata* is representative of other eukaryotic microalgae classes by their high genetic divergence. Due to the exclusive focus of this study on *C. maculata*, analyzing other species is crucial to obtain a more extensive array of data and thereby establishing general principles of purine dynamics in microalgae.

Since, to our knowledge, no other study ever emphasized the dynamics in purine formation, putting it into perspective is challenging.

Once, because many steps during accumulation, and utilization of the purine inclusions within the cell are unclear and further, their roles in symbiotic relationships, populational growth, and ecosystem dynamics are barely understood.

It has been demonstrated that uric acid formation and subsequent secretion by *Symbiodinium* sp. algae serve a symbiotic purpose in their relationship with *Aiptasia* sp. Anemones [18]. Furthermore, Kopp et al. [19] have substantiated this claim by demonstrating a swift N-uptake and subsequent translocation by *Symbiodinium* sp. to its coral host after a sudden increase in environmental nitrogen. It can thus be concluded that a symbiotic relevance for symbiotic microalgae, as the zooxanthellae, exists. However, it is not to be assumed that purines serve solely this purpose as many species that form purine-based inclusions are not reported to live in symbiotic relationships.

During the cultivation of *C. maculata* at high urea concentrations, visibly stressed cells with a paler colour and substantially lowered purine concentrations were observed. Furthermore, cultivation of *C. maculata* with NH_4^+ as the sole N-source proved unsuccessful, with all cultures perishing after a few days, even at low N-concentrations. This seems counterintuitive, given that the product of both urease-mediated urea assimilation and nitrate reduction is NH_4^+. However, it is conceivable that *C. maculata* only tolerates a limited amount of NH_4^+ and rapid, highly controlled fixation as purines therefore serves the additional purpose of N-detoxification.

Furthermore, Mojzes et al. [17] demonstrated that guanine serves as a high-capacity and rapid turnover metabolite in microalgal cells. The versatile utilization of these nitrogen reserves, combined with the rapid uptake of environmental nitrogen might thereby not just be relevant for intracellular functions, but also to support populational growth by supplying upcoming algae generations with a stock of N-metabolite.

It is therefore hypothesized that the accumulation of purines in microalgae serves a broad range of functions, combining symbiotic, metabolic, detoxifying, and possibly stress-responding purposes.

These results are thereby a novel aspect of nitrogen flux dynamics in microalgae, potentially paving the way towards new insights into symbiotic relationships, nitrogen-storage capacity, metabolic mechanisms, and/or stress responses. The application and extension of the HPLC quantification (e.g. the inclusion of pyrimidine levels and stress markers) method to other types of microalgae or other kinds of microorganisms under more diverse conditions together with a continuous monitoring (e.g. growth, physiological state) may enhance the general comprehension of nitrogen metabolism and purine formation.

CRediT authorship contribution statement

Maximilian Bott: Writing – original draft, Visualization, Validation, Methodology, Investigation, Formal analysis. **Anne Jantschke:** Writing – review & editing, Supervision, Resources, Project administration, Funding acquisition, Conceptualization.

Declaration of competing interest

The authors declare the following financial interests/personal relationships which may be considered as potential competing interests:

Anne Jantschke and Maximilian Bott report financial support was provided by German Research Foundation. If there are other authors, they declare that they have no known competing financial interests or personal relationships that could have appeared to influence the work reported in this paper.

Acknowledgements

Maximilian Bott and Anne Jantschke were financially supported by the German Research Foundation (DFG) [JA 2659/3-1]. We thank Dr. Susanne Machill, Frank Drescher, and Eike Brunner from the Bioanalytical Chemistry group at TU Dresden for their help with the HPLC-method development and for allowing us to use their HPLC instrument.

Appendix A. Supplementary data

Supplementary data to this article can be found online at https://doi.org/10.1016/j.algal.2025.104483.

Data availability

Data will be made available on request.

References

[1] W.M. Oldham, H.E. Hamm, Structural basis of function in heterotrimeric G proteins, Q. Rev. Biophys. 39 (2) (2006) 117–166, https://doi.org/10.1017/S0033583506004306.
[2] W.M. Oldham, H.E. Hamm, Heterotrimeric G protein activation by G-protein-coupled receptors, Nat. Rev. Mol. Cell Biol. (2008), https://doi.org/10.1038/nrm2299.
[3] S.R. Sprang, G protein mechanisms: insights from structural analysis, Annu. Rev. Biochem. (1997), https://doi.org/10.1146/annurev.biochem.66.1.639.
[4] K. Guille, W. Clegg, Anhydrous guanine: a synchrotron study, Acta Crystallogr. C 62 (8) (2006), https://doi.org/10.1107/S0108270106026011.
[5] A. Hirsch, et al., "Guanigma": the revised structure of biogenic anhydrous guanine, Chem. Mater. 27 (24) (2015) 8289–8297, https://doi.org/10.1021/acs.chemmater.5b03549.
[6] D. Gur, B. A. Palmer, S. Weiner, and L. Addadi, 'Light manipulation by guanine crystals in organisms: biogenic scatterers, mirrors, multilayer reflectors and photonic crystals', Feb. 10, 2017, Wiley-VCH Verlag. doi:https://doi.org/10.1002/adfm.201603514, Adv. Funct. Mater..
[7] A. F. Huxley, 'A high-power interference microscope', J. Physiol., vol. 125, no. 1, pp. 11–3P, 1954, [Online]. Available: http://europepmc.org/abstract/MED/13192775.
[8] A. Wagner, Q. Wen, N. Pinsk, and B. A. Palmer, 'Functional molecular crystals in biology', Oct. 01, 2021, John Wiley and Sons Inc. doi:https://doi.org/10.1002/ijch.202100069, Isr. J. Chem..
[9] A. Levy-Lior, et al., Guanine-based biogenic photonic-crystal arrays in fish and spiders, Adv. Funct. Mater. 20 (2) (2010) 320–329, https://doi.org/10.1002/adfm.200901437.
[10] R. De Sa, J. W. Hastings, and A. E. Vatter, 'Luminescent "crystalline" particles: an organized subcellular bioluminescent system', Science (1979), vol. 141, no. 3587, pp. 1269–1270, Sep. 1963, doi:https://doi.org/10.1126/science.141.3587.1269.
[11] R. DeSa, J.W. Hastings, The characterization of Scintillons : bioluminescent particles from the marine dinoflagellate, Gonyaulax polyedra, J. Gen. Physiol. 51 (1) (1968) 105–122, https://doi.org/10.1085/jgp.51.1.105.
[12] R.E. Schmitter, The fine structure of Gonyaulax polyedra, a bioluminescent marine dinoflagellate, J. Cell Sci. 9 (1) (1971) 147–173, https://doi.org/10.1242/jcs.9.1.147.
[13] C.E. Creutz, S. Mohanty, T. Defalco, R. Kretsinger, Purine composition of the crystalline cytoplasmic inclusions of Paramecium tetraurelia, Protist 153 (1) (2002) 39–45, https://doi.org/10.1078/1434-4610-00081.
[14] Š. Moudříková, L. Nedbal, A. Solovchenko, P. Mojzeš, Raman microscopy shows that nitrogen-rich cellular inclusions in microalgae are microcrystalline guanine, Algal Res. 23 (2017) 216–222, https://doi.org/10.1016/j.algal.2017.02.009.
[15] J. Pilátová, T. Pánek, M. Oborník, I. Čepička, P. Mojzeš, Revisiting biocrystallization: purine crystalline inclusions are widespread in eukaryotes, ISME J. 16 (9) (2022) 2290–2294, https://doi.org/10.1038/s41396-022-01264-1.
[16] A. Jantschke, et al., Anhydrous β-guanine crystals in a marine dinoflagellate: structure and suggested function, J. Struct. Biol. 207 (1) (2019) 12–20, https://doi.org/10.1016/j.jsb.2019.04.009.
[17] P. Mojzeš, et al., Guanine, a high-capacity and rapid-turnover nitrogen reserve in microalgal cells, PNAS 117 (51) (2020) 32722–32730, https://doi.org/10.1073/pnas.2005460117/-/DCSupplemental.
[18] P.L. Clode, M. Saunders, G. Maker, M. Ludwig, C.A. Atkins, Uric acid deposits in symbiotic marine algae, Plant Cell Environ. 32 (2) (2009) 170–177, https://doi.org/10.1111/j.1365-3040.2008.01909.x.
[19] C. Kopp, et al., Highly dynamic cellular-level response of symbiotic coral to a sudden increase in environmental nitrogen, mBio 4 (3) (2013), https://doi.org/10.1128/mBio.00052-13.
[20] N. Pinsk, et al., Biogenic guanine crystals are solid solutions of guanine and other purine metabolites, J. Am. Chem. Soc. 144 (11) (2022) 5180–5189, https://doi.org/10.1021/jacs.2c00724.
[21] K.G. Wagner, A.I. Backer, Dynamics of nucleotides in plants studied on a cellular basis, in: International Review of Cytology 134, Elsevier, 1992, pp. 1–84, https://doi.org/10.1016/S0074-7696(08)62027-6.
[22] G.D. van der Vogels, C. Van der Drift, Degradation of purines and pyrimidines by microorganisms, Bacteriol. Rev. 40 (2) (1976) 403–468.
[26] C. Hou, G. Xiao, W. Amakye, J. Sun, Z. Xu, and J. Ren, 'Guidelines for purine extraction and determination in foods', Food Front, vol. 2, Jun. 2021, doi:https://doi.org/10.1002/fft2.100, Food Front..
[27] M.G. Simic, S.V. Jovanovic, Antioxidation mechanisms of uric acid, J. Am. Chem. Soc. 111 (15) (1989) 5778–5782.

[28] R. Dalpozzo, G. Bartoli, L. Sambri, P. Melchiorre, Perchloric acid and its salts: very powerful catalysts in organic chemistry, Chem. Rev. 110 (6) (2010) 3501–3551, https://doi.org/10.1021/cr9003488.
[29] J. Sharma, et al., Effect of different nitrogen sources on growth of algal consortia, Ann. Agri-Bio Res. 22 (2) (2017) 150–153.
[30] S.O. Lourenço, E. Barbarino, J. Mancini-Filho, K.P. Schinke, E. Aidar, Effects of different nitrogen sources on the growth and biochemical profile of 10 marine microalgae in batch culture: an evaluation for aquaculture, Phycologia 41 (2) (2002) 158–168, https://doi.org/10.2216/i0031-8884-41-2-158.1.
[31] G. Sinclair, D. Kamykowski, P.M. Glibert, Growth, uptake, and assimilation of ammonium, nitrate, and urea, by three strains of Karenia brevis grown under low light, Harmful Algae 8 (5) (2009) 770–780, https://doi.org/10.1016/j.hal.2009.02.006.
[32] T. Berman, S. Chava, Algal growth on organic compounds as nitrogen sources, J. Plankton Res. 21 (8) (1999) 1423–1437, https://doi.org/10.1093/plankt/21.8.1423.
[33] N.J. Antia, B.R. Berland, D.J. Bonin, S.Y. Maestrini, Effects of urea concentration in supporting growth of certain marine microplanktonic algae, Phycologia 16 (1) (1977) 105–111, https://doi.org/10.2216/i0031-8884-16-1-105.1.
[34] K.J. Erratt, I.F. Creed, C.G. Trick, Comparative effects of ammonium, nitrate and urea on growth and photosynthetic efficiency of three bloom-forming cyanobacteria, Freshw. Biol. 63 (7) (2018) 626–638, https://doi.org/10.1111/fwb.13099.
[35] L.F. Wu, P.C. Chen, C.M. Lee, The effects of nitrogen sources and temperature on cell growth and lipid accumulation of microalgae, Int. Biodeterior. Biodegradation 85 (2013) 506–510, https://doi.org/10.1016/j.ibiod.2013.05.016.
[36] J.P. Fidalgo, A. Cid, E. Torres, A. Sukenik, C. Herrero, Effects of nitrogen source and growth phase on proximate biochemical composition, lipid classes and fatty acid profile of the marine microalga Isochrysis galbana, Aquaculture 166 (1) (1998) 105–116, https://doi.org/10.1016/S0044-8486(98)00278-6.
[37] A.D. Batista, et al., Increased urea availability promotes adjustments in C/N metabolism and lipid content without impacting growth in *Chlamydomonas reinhardtii*, Metabolomics 15 (3) (2019) 31, https://doi.org/10.1007/s11306-019-1496-3.
[38] I. Gifuni, G. Olivieri, A. Pollio, A. Marzocchella, Identification of an industrial microalgal strain for starch production in biorefinery context: the effect of nitrogen and carbon concentration on starch accumulation, New Biotechnol. 41 (2018) 46–54, https://doi.org/10.1016/j.nbt.2017.12.003.
[39] S. Zhu, et al., Enhanced accumulation of carbohydrate and starch in Chlorella zofingiensis induced by nitrogen starvation, Appl. Biochem. Biotechnol. 174 (7) (2014) 2435–2445, https://doi.org/10.1007/s12010-014-1183-9.
[40] G. Dragone, B.D. Fernandes, A.P. Abreu, A.A. Vicente, J.A. Teixeira, Nutrient limitation as a strategy for increasing starch accumulation in microalgae, Appl. Energy 88 (10) (2011) 3331–3335, https://doi.org/10.1016/j.apenergy.2011.03.012.
[41] J. Abalde, J. Fabregas, C. Herrero, B-Carotene, vitamin C and vitamin E content of the marine microalga Dunaliella tertiolecta cultured with different nitrogen sources, Bioresour. Technol. 38 (2) (1991) 121–125, https://doi.org/10.1016/0960-8524(91)90142-7.
[42] J. Chen, X. Jiang, D. Wei, Effects of urea on cell growth and physiological response in pigment biosynthesis in mixotrophic Chromochloris zofingiensis, J. Appl. Phycol. 32 (3) (2020) 1607–1618, https://doi.org/10.1007/s10811-020-02114-3.
[43] D.M. Anderson, P.M. Glibert, J.M. Burkholder, Harmful algal blooms and eutrophication: nutrient sources, composition, and consequences, Estuaries 25 (2002) 704–726, https://doi.org/10.1007/BF02804901.
[44] L.W. Little, R.A. Mah, Ammonia production in urea-grown cultures of Chlorella Ellipsoidea, J. Phycol. 6 (3) (1970) 277–280, https://doi.org/10.1111/j.1529-8817.1970.tb02393.x.
[45] J.W. Leftley, P.J. Syrett, Urease and ATP: urea amidolyase activity in unicellular algae, Microbiology (N Y) 77 (1) (1973) 109–115, https://doi.org/10.1099/00221287-77-1-109.
[46] R.K. Allison, H.E. Skipper, M.R. Reid, W.A. Short, G.L. Hogan, Sodium formate and urea feeding experiments with Nostoc muscorum, Plant Physiol. 29 (2) (1954) 164, https://doi.org/10.1104/pp.29.2.164.
[47] D. S. Berns, P. Holohan, and E. Scott, 'Urease activity in blue-green algae', Science (1979), vol. 152, no. 3725, pp. 1077–1078, 1966, doi:https://doi.org/10.1126/science.152.3725.1077.
[48] N.S.T. Lui, O.A. Roels, The assimilation and formation of urea in Ochromonas malhamensis, Arch. Biochem. Biophys. 139 (2) (1970) 269–277, https://doi.org/10.1016/0003-9861(70)90478-9.
[49] R.A. Pecora, R.G. Rhodes, A comparative study of growth in Bumilleriopsis filiformis, B. Peterseniana, and Pseudobumilleriopsis pyrenoidosa (Xanthophyceae), Can. J. Bot. 50 (2) (1972) 337–341, https://doi.org/10.1139/b72-046.
[50] W.H. Thomas, R.W. Krauss, Nitrogen metabolism in Scenedesmus as affected by environmental changes, Plant Physiol. 30 (2) (1955) 113, https://doi.org/10.1104/pp.30.2.113.
[51] A. Hattori, Studies on the metabolism of urea and other nitrogenous compounds in Chlorella ellipsoidea II. Changes on levels of amino acids and amides during the assimilation of ammonia and urea by nitrogen-starved cells, The Journal of Biochemistry 45 (1) (1958) 57–64, https://doi.org/10.1093/oxfordjournals.jbchem.a126800.
[52] A. Hattori, Studies on the metabolism of urea and other nitrogenous compounds in Chlorella ellipsoidea I. Assimilation of urea and other nitrogenous compounds by nitrogen-starved cells, The journal of Biochemistry 44 (5) (1957) 253–273, https://doi.org/10.1093/oxfordjournals.jbchem.a126752.
[53] J.B. Walker, Arginosuccinic acid from Chlorella, Proc. Natl. Acad. Sci. 38 (7) (1952) 561–566, https://doi.org/10.1073/pnas.38.7.561.
[54] S.R. Johnson, Urea Metabolism by the Marine Cryptomonad *Rhodomonas lens*, University of british columbia, Ottawa, 1971.
[55] M. Daudon, M.F. Protat, R.J. Reveillaud, H. Jaeschke-Boyer, Infrared spectrometry and Raman microprobe in the analysis of urinary calculi, Kidney Int. 23 (6) (1983) 842–850, https://doi.org/10.1038/ki.1983.104.
[56] Venkata Ramana Kodati, Anthony T Tu, Jacob L Turumin, Raman spectroscopic identification of uric-acid-type kidney stone, Appl. Spectrosc. 44 (7) (1990) 1134–1136, https://doi.org/10.1366/0003702904086470.
[57] T. Soare, et al., Identification of uric acid crystals accumulation in human and animal tissues using combined morphological and Raman spectroscopy analysis, Diagnostics 12 (11) (2022), https://doi.org/10.3390/diagnostics12112762.
[58] J.-W. Zhou, et al., Reliable quantitative detection of uric acid in urine by surface-enhanced Raman spectroscopy with endogenous internal standard, Biosens. Bioelectron. 251 (2024) 116101, https://doi.org/10.1016/j.bios.2024.116101.